

# Further Pseudopericyclic Reactions: An *ab Initio* Study of the Conformations and Reactions of 5-Oxo-2,4-pentadienal and Related Molecules

David M. Birney

Department of Chemistry and Biochemistry, Texas Tech University, Lubbock, Texas 79409-1061

Received September 19, 1995<sup>©</sup>

It has been proposed that all pseudopericyclic reactions are allowed, regardless of the number of electrons involved. 5-Oxo-2,4-pentadienal (**1**) is a vinylog of formylketene, and thus its reactions provide a test of this proposal. *Ab initio* (MP4(full, SDQ)/D95\*\*//MP2/6-31G\* + ZPE) calculations were carried out on all the conformations and several reactions of **1**, as well as related systems. One of the eight possible conformations of **1** (zZz1) does not exist, but closes without a barrier, via a pseudopericyclic pathway to pyran-2-one (**3**). IR spectra of **1** in Ar matrices are consistent with three conformations (zZe1, eZz1, and eZe1). Calculated rotational barriers from zZe1 and eZz1 to **3** are consistent with observed kinetics for the decay of **1**. The structures of *s*-*Z*- and *s*-*E*-3-hydroxy-1,2-propadien-1-one (**18** and **19**) and the vinylogous cumulene **16** are predicted to have strongly bent geometries. The barrier to internal proton transfer from **16** is only 0.8 kcal/mol, while the barrier from **18** is 23.7 kcal/mol. Barrier heights for these and other pseudopericyclic reactions are shown to correlate with (1) the nucleophilicity and electrophilicity of the reacting centers, (2) the exothermicity of the reaction, and (3) deviations from the ideal geometries for the reaction. Significantly, the barrier heights do *not* correlate with the number of electrons involved in the reaction.

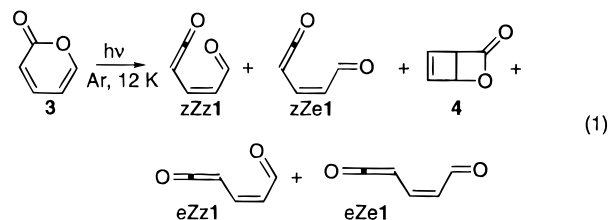
## Introduction

5-Oxo-2,4-pentadienal (**1**)<sup>1</sup> is a vinylog of formylketene (**2**), and as such its reactions are expected to provide an informative contrast to those of the latter, which have been more extensively studied.<sup>2</sup> Because of our own interest in the reactions of  $\alpha$ -oxoketenes and in particular, Lemal's<sup>3</sup> and our prediction that all pseudopericyclic reactions are orbital symmetry allowed, regardless of the number of electrons participating in the reaction,<sup>4,5</sup> we undertook the study of **1** described below.



Direct evidence for the title ketene **1** has been obtained from matrix isolation photochemistry of pyran-2-one (**3**)<sup>1a,b</sup> (eq 1). The IR absorptions in the aldehyde (1760

cm<sup>-1</sup>) and ketene regions (2146, 2136, 2129, and 2122 cm<sup>-1</sup>) of the spectra were assigned by Chapman et al.,<sup>1a</sup> and independently by Pong and Shirk,<sup>1b</sup> as the four single bond rotamers of ketene **1** which are possible while maintaining the *Z* conformation of the 3–4 double bond.<sup>7</sup> Changes in the spectra upon further photolysis and/or warming the matrix were attributed to rotational interconversion of several of the isomers.<sup>8</sup> The conformations of **1** are described herein as *s*-*Z* or *s*-*E* about the C<sub>2</sub>–C<sub>3</sub> single bond (designated as *z* or *e*), *Z* or *E* about the C<sub>3</sub>–C<sub>4</sub> double bond, and *s*-*Z* or *s*-*E* about the C<sub>4</sub>–C<sub>5</sub> single bond. Thus the four conformations previously assigned in the matrix spectra are zZz1, zZe1, eZz1, and eZe1 (eq 1).



Ketene **1** was subsequently implicated as a reactive intermediate in the thermal rearrangement of substituted pyranones such as 5-methylpyran-2-one (**5**) to give 3-methylpyran-2-one (**8**).<sup>1c</sup> Oxygen-18 labeling studies

<sup>©</sup> Abstract published in *Advance ACS Abstracts*, November 15, 1995.

(1) (a) Chapman, O. L.; McIntosh, C. L.; Pacansky, J. *J. Am. Chem. Soc.* **1973**, *95*, 244–246. (b) Pong, R. G. S.; Shirk, J. S. *J. Am. Chem. Soc.* **1973**, *95*, 248–249. (c) Pirkle, W. H.; Turner, W. V. *J. Org. Chem.* **1975**, *40*, 1617–1620. (d) Bell, G. A.; Dunkin, I. R. *J. Chem. Soc., Chem. Commun.* **1983**, 1213–1215. (e) Chapman, O. L.; Hess, T. C. *J. Am. Chem. Soc.* **1984**, *106*, 1842–1843. (f) Arnold, B. R.; Brown, C. E.; Luszyk, J. *J. Am. Chem. Soc.* **1993**, *115*, 1576–1577.

(2) (a) Kaneko, C.; Sato, M.; Sakaki, J.-i.; Abe, Y. *J. Heterocycl. Chem.* **1990**, *27*, 25. (b) Kappe, C. O.; Evans, R. A.; Kennard, C. H. L.; Wentrup, C. *J. Am. Chem. Soc.* **1991**, *113*, 4234–4237. (c) Allen, A. D.; Andaos, J.; Kresge, A. J.; McAllister, M. A.; Tidwell, T. T. *J. Am. Chem. Soc.* **1992**, *114*, 1878–1879. (d) Leung-Toung, R.; Wentrup, C. *Tetrahedron* **1992**, *48*, 7641–7654. (e) Wentrup, C.; Heilmayer, W.; Kollenz, G. *Synthesis* **1994**, 1219–1248. (f) Hyatt, J. A.; Reynolds, P. W. In *Organic Reactions*; L. A. Paquette, Ed.; John Wiley & Sons, Inc.: 1994; Vol. 45; pp 159–635. (g) Kappe, C. O.; Wong, M. W.; Wentrup, C. *J. Org. Chem.* **1995**, *60*, 1686–1695.

(3) Ross, J. A.; Seiders, R. P.; Lemal, D. M. *J. Am. Chem. Soc.* **1976**, *98*, 4325–4327.

(4) (a) Ham, S.; Birney, D. M. *Tetrahedron Lett.* **1994**, *35*, 8113–8116. (b) Birney, D. M.; Wagenseller, P. E. *J. Am. Chem. Soc.* **1994**, *116*, 6262–6270. (c) Birney, D. M. *J. Org. Chem.* **1994**, *59*, 2557–2564. (d) Wagenseller, P. E.; Birney, D. M.; Roy, D. *J. Org. Chem.* **1995**, *60*, 2853–2859.

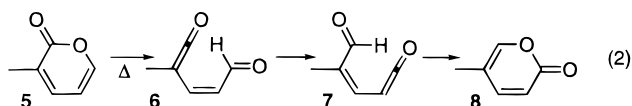
(5) Pseudopericyclic reactions were originally defined by Lemal as pericyclic reactions in which there is a disconnection in the cyclic array of overlapping orbitals, because of the presence of orthogonal orbital systems. Wentrup<sup>6</sup> has also suggested that the presence of orthogonal orbitals could make an otherwise forbidden 1,3-sigmatropic shift allowed.

(6) Wentrup, C.; Netsch, K. P. *Angew. Chem., Int. Ed. Engl.* **1984**, *23*, 802.

(7) It appears that there is a fifth distinct ketene peak in the published spectrum Figure 2a in reference 1a at 2138 cm<sup>-1</sup>.

(8) Recent studies on the matrix isolation IR spectroscopy of acetylketene suggest that photochemical rotational interconversion is possible, but that multiple matrix sites can lead to multiple absorptions from a single isomer, and the sites can be interconverted by warming.<sup>2g</sup>

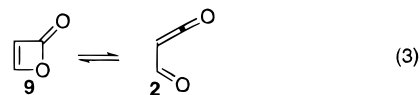
were consistent with the 1,5-hydrogen shift of **6** to **7** shown in eq 2. Ketene **1** is also observed in the matrix isolation photolysis of the carbonyl oxide, cyclopentadienone *O*-oxide.<sup>1d,e</sup>



More recently, Arnold, Brown, and Luszyk<sup>1f</sup> have reported a room temperature, time-resolved IR study of the photochemistry of **3**. Laser flash photolysis of **3** generated ketene **1** and the lactone **4**, respectively. (Absorptions due to different rotamers of **1** could not have been resolved, due to instrumental limitations and solution broadening.) The signal from **1** decayed with first-order kinetics and a lifetime of 2.9  $\mu$ s. Concurrently, the absorption due to **3** recovered, indicating the thermal reversion of **1** to **3**.

$\alpha$ -Oxoketenes have been intensively studied<sup>2,9</sup> and this work has been the subject of two recent reviews.<sup>2e,f</sup> *Ab initio* calculations from this laboratory,<sup>4a,b,d</sup> as well as others,<sup>10</sup> indicate that the transition states for cycloadditions, electrocyclizations, and sigmatropic rearrangements of  $\alpha$ -oxoketenes are all essentially planar, in contrast to the distinctly nonplanar transition states calculated for hydrocarbon pericyclic reactions.<sup>11</sup> The planarity of these transition structures prevents overlap of the  $\sigma$ - and  $\pi$ -orbitals, in what Lemal has defined as a pseudopericyclic orbital topology.<sup>3</sup> Note that the presence of one or more carbonyls in a pericyclic system is not sufficient to permit a planar, and hence pseudopericyclic, transition state. For example, hetero Diels–Alder reactions<sup>12</sup> and the ring openings of oxetone<sup>13</sup> or 1,2-cyclobutenedione<sup>14</sup> all have nonplanar transition structures.<sup>15</sup>

Furthermore, pseudopericyclic reactions may have low activation energies due to the lack of electron–electron repulsion enforced by a pericyclic orbital array.<sup>4a,b,d,17</sup> For example, [4 + 2] cycloadditions of  $\alpha$ -oxoketenes are usually more facile than the [2 + 2] reactions commonly associated with ketenes.<sup>2e,f,4a,b,d</sup> *Ab initio* calculations suggest that the planar electrocyclic ring opening of oxetone **9** to **2** occurs with a very low barrier of only 2.5 kcal/mol (eq 3).<sup>4b,10a</sup> A planar transition state is calculated for the degenerate 1,3-sigmatropic hydrogen shift in formylketene.<sup>10a,c</sup>



Finally, the lack of cyclic overlap has the remarkable consequence that for a pseudopericyclic orbital topology, a reaction is orbital symmetry allowed, regardless of the number of electrons involved.<sup>4a,b,d</sup> Therefore one may make two bold predictions. The 1,5-hydrogen migration observed in ketene **6** (eq 2) could proceed via a planar, pseudopericyclic transition state and be orbital symmetry allowed just as is the 1,3-hydrogen migration calculated for formylketene (**2**).<sup>10a</sup> Similarly, the ring closure of the *zZz* conformer of **1** would be expected to be an allowed reaction, with both a potentially low barrier and a planar transition state, in analogy to that calculated for the ring opening of oxetone **9** (eq 3).<sup>4b,10a</sup> (Orbital diagrams for these two reactions are provided in Figure 1 of the supporting information.) Therefore, this study was begun by searching for transition structures for these two reactions, the ring closure of *zZz1* and the degenerate 1,5-hydrogen shift in *zZe1*.

### Computational Methods

The *ab initio* molecular orbital calculations were carried out using Gaussian 92.<sup>18</sup> Geometry optimizations were performed first at the RHF/6-31G\* level and then at the MP2(FC)/6-31G\* level. Single determinant wavefunctions such as RHF/6-31G\* calculations usually qualitatively reproduce transition structures for orbital symmetry allowed (but not forbidden) pericyclic reactions.<sup>11</sup> Frequency calculations at each optimized geometry verified the identity of each stationary point as a minimum or transition state. Single point energies of each structure were obtained at the MP4(full, SDQ)/D95\*\* level. The zero-point vibrational energy (ZPE) corrections were obtained by scaling the MP2/6-31G\* ZPE by 0.9646, as recommended by Pople et al.<sup>19</sup> Unless otherwise indicated, all energies discussed in the text are MP4(SDQ, full)/D95\*\* with the ZPE correction. Absolute energies are reported in Table 2 of the supporting information. Relative energies, lowest or imaginary frequencies, ZPE's, and dipole moments are reported in Table 1. Ketene and carbonyl frequencies (scaled by 0.960<sup>2g</sup> and 0.9427,<sup>19</sup> respectively) for conformations of **1** are given in Table 2, while frequencies scaled by 0.9427<sup>19</sup> for **18** and **19** are in Table 3. Selected data for optimized geometries are shown in Figures 1–3; full geometries and vibrational frequencies are available in the supporting information. Atom numbering is as shown in Figure 1 for **3**.

The D95\*\* basis set (a double  $\zeta$  basis set with independent s and p coefficients and with polarization functions on all atoms)<sup>20</sup> was used for single point energies. In two cases (planar and nonplanar **15**) MP4(full, SDQ)

(9) (a) Nikolaev, V. A.; Frenkh, Y.; Korobitsyna, I. K. *J. Org. Chem. USSR (Eng. Transl.)* **1978**, *14*, 1069–1079. (b) Maier, G.; Reisenauer, H. P.; Sayrac, T. *Chem. Ber.* **1982**, *115*, 2192–2201. (c) Kappe, C. O.; Farber, G.; Wentrup, C.; Kollenz, G. *J. Org. Chem.* **1992**, *57*, 7078–7083.

(10) (a) Nguyen, M. T.; Ha, T.; More O'Ferrall, R. A. *J. Org. Chem.* **1990**, *55*, 3251–3256. (b) Allen, A. D.; McAllister, M. A.; Tidwell, T. T. *Tetrahedron Lett.* **1993**, *34*, 1095–1098. (c) Wong, M. W.; Wentrup, C. *J. Org. Chem.* **1994**, *59*, 5279–5285. (d) Hong, S. G.; Fu, X. Y. *J. Mol. Struct. (THEOCHEM)* **1990**, *209*, 241.

(11) Houk, K. N.; Li, Y.; Evansck, J. D. *Angew. Chem., Int. Ed. Engl.* **1992**, *31*, 682–708.

(12) McCarrick, M. A.; Wu, Y.-D.; Houk, K. N. *J. Am. Chem. Soc.* **1992**, *114*, 1499–1500.

(13) Kallel, E. A.; Wang, Y.; Houk, K. N. *J. Org. Chem.* **1989**, *54*, 6006.

(14) Allen, A. D.; Colomvakos, J. D.; Egle, I.; Luszyk, J.; McAllister, M. A.; Tidwell, T. T.; Wagner, B. D.; Zhao, D.-c. *J. Am. Chem. Soc.* **1995**, *117*, 7552–7553.

(15) Iminoketenes are also capable of undergoing planar, pseudopericyclic reactions, in analogy to  $\alpha$ -oxoketenes.<sup>16</sup> However, vinylketenes, lacking lone pairs at both ends, will only undergo pericyclic reactions.

(16) Eisenberg, S. W. E.; Kurth, M. J.; Fink, W. H. *J. Org. Chem.* **1995**, *60*, 3736–3742.

(17) Houk, K. N.; Gandour, R. W.; Strozier, R. W.; Rondan, N. G.; Paquette, L. A. *J. Am. Chem. Soc.* **1979**, *101*, 6797–6802.

(18) Frisch, M. J.; Trucks, G. W.; Head-Gordon, M.; Gill, P. M. W.; Wong, M. W.; Foresman, J. B.; Johnson, B. G.; Schlegel, H. B.; Robb, M. A.; Replogle, E. S.; Gomperts, R.; Andres, J. L.; Raghavachari, K.; Binkley, J. S.; Gonzalez, C.; Martin, R. L.; Fox, D. J.; Defrees, D. J.; Baker, J.; Stewart, J. J. P.; Pople, J. A. Gaussian, Inc. Pittsburgh, PA, 1992.

(19) Pople, J. A.; Scott, A. P.; Wong, M. W.; Radom, L. *Isr. J. Chem.* **1993**, *33*, 345.

(20) Dunning, T. H.; Hay, P. J. *Modern Theoretical Chemistry*; Plenum: New York, 1976.

**Table 1. Relative Energies (kcal/mol), Low or Imaginary Frequencies, Zero Point Vibrational Energies (ZPE), and Dipole Moments of Structures Optimized at the MP2/6-31G\* Level**

structure	RHF/ 6-31G*	MP2/ 6-31G* fc <sup>a</sup>	low freq <sup>b</sup>	ZPE <sup>c</sup>	dipole moment <sup>d</sup>	RHF/ d95**	MP2/ D95**	MP3/ D95**	MP4 SDQ/ D95**	MP4 SDTQ/ D95**	MP4 SDQ + ΔZPE <sup>e</sup>	MP4 SDTQ + ZDPE <sup>e</sup>
<b>C<sub>5</sub>H<sub>4</sub>O<sub>2</sub>, Energies Relative to <b>3</b></b>												
<b>3</b>	0.0	0.0	141.5	50.7	5.43	0.0	0.0	0.0	0.0	0.0	0.0	0.0
zZz1 <sup>f</sup>			107.4	52.3	3.63							
zZe1	30.6	30.2	66.1	48.3	5.14	31.2	30.3	32.4	28.8		26.5	
eZz1	25.3	25.2	101.1	48.6	2.83	25.9	25.7	28.2	24.7		22.7	
eZe1	25.3	28.3	70.8	48.3	3.26	27.8	28.1	30.1	26.5		24.2	
zEz1	26.7	27.6	49.2	48.3	2.81	27.7	28.4	30.6	26.9		24.6	
zEe1	26.2	26.8	86.5	48.3	5.22	26.6	26.9	29.1	25.5		23.2	
eEz1	24.9	26.0	99.6	48.5	3.95	25.8	26.9	29.0	25.4		23.2	
eEe1	24.5	25.5	82.9	48.3	3.56	24.8	25.7	27.7	24.3		22.0	
<b>4</b>	44.6	39.3	161.7	50.5	4.99	43.1	37.9	37.6	36.5		36.2	
<b>10</b>	36.9	37.8	-178.2	47.7	3.90	37.6	38.0	38.6	35.0	35.4	32.0	32.5
<b>11</b>	37.5	37.0	-197.1	47.7	4.53	38.1	36.9	38.3	34.4	34.6	31.5	31.7
<b>12</b>	33.2	33.1	90.6	49.0	3.40	32.4	32.2	32.0	29.5		27.9	
<b>13</b>	66.5	54.2	-533.9	47.8	4.07	68.0	54.7	62.3	58.0		55.2	
<b>14</b>	64.6	53.7	-607.1	47.9	4.02	65.4	53.8	60.6	56.8		54.1	
<b>15 planar</b>	72.9	49.72	-423.9, -131.1	46.0	4.51	72.9	46.9	61.4	54.7		50.2	
<b>15</b>	73.1	49.69	-415.5	46.4	4.55	73.0	47.0	61.3	54.8	43.4	50.6	39.2
<b>15<sup>g</sup></b>	0.2	-0.11	-137.1	46.4	4.78	-0.1	-0.1	0.2	-0.3			
<b>16</b>	53.7	43.2	118.1	49.1	4.07	51.1	40.6	48.1	45.9		44.3	
<b>17</b>	59.9	45.2	-1376.5	46.3	3.95	57.7	42.4	52.9	49.4		45.2	
<b>C<sub>3</sub>H<sub>2</sub>O<sub>2</sub>, Energies Relative to <b>2</b></b>												
<b>2</b>	0.0	0.0	150.5	27.1	2.37	0.0	0.0	0.0	0.0	0.0	0.0	0.0
<b>18</b>	28.1	21.4	142.4	28.0	2.28	25.2	18.9	21.3	22.9	19.3	23.8	20.2
<b>19</b>	34.3	27.2	144.8	27.7	5.12	31.5	24.7	26.6	28.4	25.0	29.0	25.6
<b>20</b>	74.4	54.3	-1985.2	24.2	1.83	72.1	52.4	61.5	59.7	52.8	56.9	50.0
<b>CH<sub>2</sub>O<sub>2</sub>, Energies Relative to Formic Acid</b>												
formic acid	0.0	0.0	626.8	21.5	1.59	0.0	0.0	0.0	0.0	0.0	0.0	0.0
<b>22</b>	51.0	35.4	-1894.3	18.5	1.35	50.9	35.8	42.1	39.5	36.3	36.6	33.5

<sup>a</sup> Frozen core. <sup>b</sup> In cm<sup>-1</sup>. Negative numbers indicate imaginary frequencies. <sup>c</sup> In kcal/mol, unscaled, from MP2/6-31G\* frequencies. <sup>d</sup> In Debye, at the MP2/6-31G\* geometry. All other MP calculations were performed using all electrons. <sup>e</sup> With the D95\*\* basis set. ZPE's were from MP2/6-31G\* frequencies, scaled by 0.9646, as recommended in reference 19. <sup>f</sup> At the RHF/6-31G\* geometry. This was not a stationary point at the MP2/6-31G\* level. See text for details. <sup>g</sup> Calculated with the 6-31++G\*\* basis set at the MP2/6-31++G\*\* geometry. Energies are relative to **15 planar**.

calculations were also carried out with the larger 6-31++G\*\* basis set. The D95\*\* basis set gave significantly lower absolute RHF energies than either the 6-31G\* or 6-31++G\*\* basis sets (Table 2, supporting information). The calculations were generally terminated at the MP4(full, SDQ)/D95\*\* level because of the limitations of disk space and computational time available, although for smaller molecules and for selected larger molecules the triple excitations were included in the MP4 calculations. Inclusion of the triples lowered the absolute energies significantly as compared to MP4-(SDQ) energies. In some cases (**2**, **15**, **18**, **19**, and **20**) the triples also tended to lower the energies of the reactive intermediates and transition states relative to the global minima, although the energy orderings did not change (Table 1). In other cases (**3**, **10**, **11**, and **22**) the relative energies were unchanged. The core orbitals were included in the calculations to recover a small additional correlation correction.

## Results and Discussion

**Conformations of 1.** Optimizations of pyran-2-one (**3**), the bicyclic lactone **4**, and seven of the eight conformations of ketene **1** were straightforward at both the RHF/6-31G\* and MP2/6-31G\* levels. These structures and their relative energies are shown in Scheme 1. These were planar, with the exceptions of **4** (as expected) and zZe1, which was slightly nonplanar.<sup>21</sup> The ring strain in lactone **4** places it 14.3 kcal/mol higher in energy than the most stable conformer of **1**.

However, zZz1, which was of interest in terms of the ring closure, is apparently not a stable molecule. The geometry of zZz1 was optimized at the RHF/6-31G\* level (Figure 1), and an early and planar transition state for ring closure to **3** was located and characterized by a frequency calculation at the same level. The barrier height for ring closure is only 1.5 kcal/mol at this level and should be even lower with the ZPE correction. In this structure for zZz1, the O-C-C angle of 167.2° and the C<sub>1</sub>-O<sub>5</sub> distance of 2.417 Å, only 1.0 Å longer than in **3**, indicate that there is substantial covalent bonding between C<sub>1</sub> and O<sub>5</sub>. All attempts to optimize the geometry of zZz1 at the MP2/6-31G\* level led to the pyran-2-one (**3**). Because the previous experimental studies had assumed that this was one of the conformations observed,<sup>1a,b,f</sup> it was important to verify that there was indeed no barrier at this, or higher levels of theory. Since it was not practical to attempt geometry optimizations at a higher level, a series of partial MP2/6-31G\* optimizations were carried out, in which the C<sub>1</sub>-O<sub>5</sub> bond was held fixed and the rest of the molecule optimized at the MP2/6-31G\* level. MP4(SDQ)/6-31G\* single point energies were then calculated at each geometry. These

(21) We are reasonably confident that these structures are indeed planar, because the MP2/6-31G\* calculations can predict a gauche conformation, as is the case for 1,3-butadiene.<sup>22</sup> However, we do not attach much significance to the strict planarity or lack thereof in these systems, in view of the experimental and theoretical difficulties in determining whether or not *s-cis* butadiene is planar or gauche.<sup>22,23</sup>

(22) Wiberg, K. B.; Rosenberg, R. E. *J. Am. Chem. Soc.* **1990**, *112*, 1509-1519.

(23) Arnold, B. R.; Balaji, V.; Michl, J. *J. Am. Chem. Soc.* **1990**, *112*, 1808-1812.

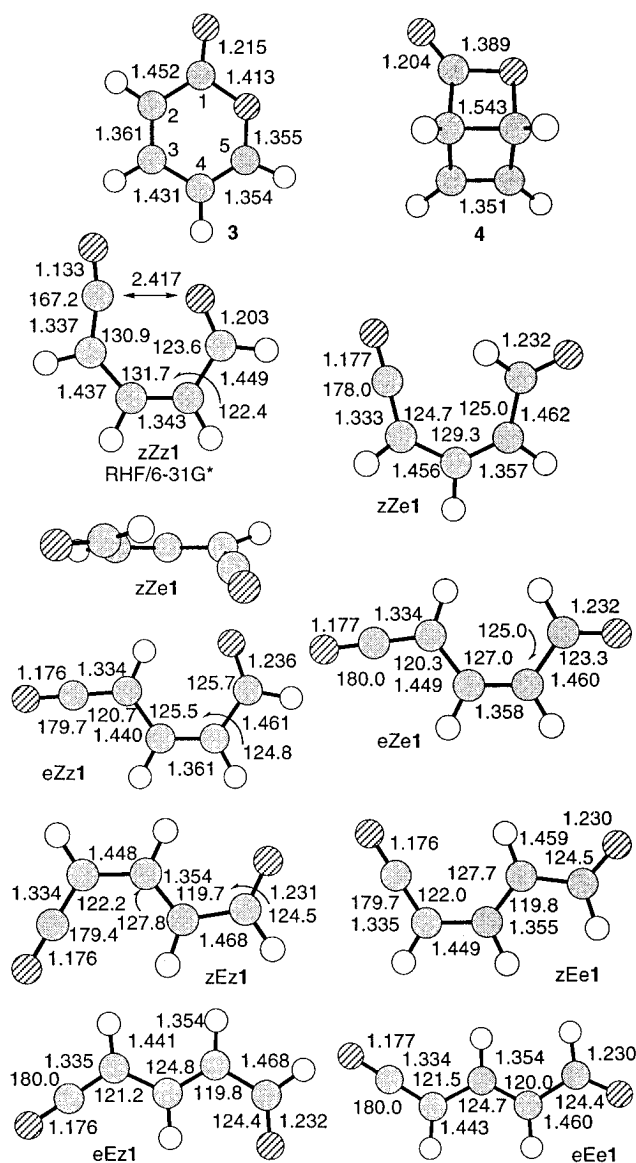


**Figure 1.** MP2/6-31G\* optimized geometries of pyran-2-one (**3**), lactone **4**, and the eight conformations of **1**. Carbons are shaded, oxygens are striped and hydrogens are open. Distances are in angstroms and angles in degrees. All structures except **4** and zZe1 are planar. Note that the structure shown for zZz1 was obtained at the RHF/6-31G\* level. It is not a stationary point at the MP2/6-31G\* level. The O<sub>1</sub>-C<sub>1</sub>-O<sub>5</sub> angle in zZz1 is 97.3°. Dihedral angles in zZe1 are C<sub>1</sub>-C<sub>2</sub>-C<sub>3</sub>-C<sub>4</sub> = 26.4°, C<sub>2</sub>-C<sub>3</sub>-C<sub>4</sub>-C<sub>5</sub> = 7.3°, C<sub>3</sub>-C<sub>4</sub>-C<sub>5</sub>-H<sub>5</sub> = 8.2°.

structures were all planar; distortions out of the plane raised the energy. The relative energies calculated at various levels are plotted in Figure 4; the absolute energies are reported in the supporting information. Although the flatness of the plateau on the potential energy surface depends on the level of theory, at none of the correlated levels is there a minimum in the vicinity of the RHF/6-31G\* structure for zZz1.

It may be surprising that a reasonable looking closed shell molecule such as zZz1 might not exist. However it is common for calculated barrier heights to be lower at the MP2/6-31G\* level than at the RHF level. There are four additional factors which together eliminate this barrier. First, there is an orbital symmetry allowed, pseudopericyclic pathway available. Second, there is a good match between the nucleophilic aldehyde oxygen and electrophilic ketene carbon of zZz1 which favors the

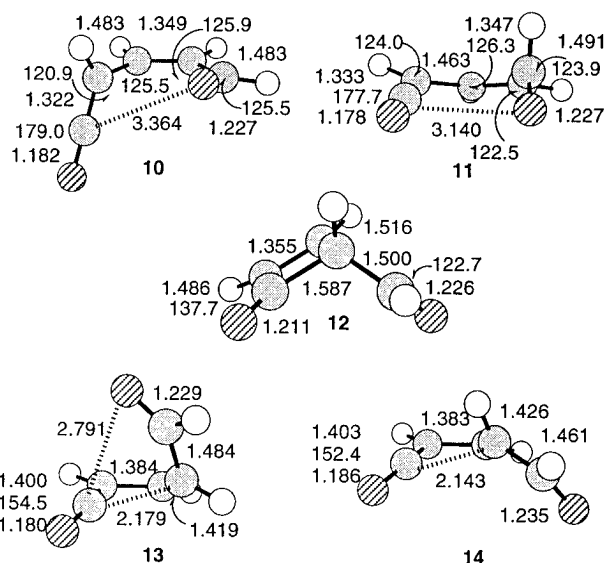


**Figure 2.** MP2/6-31G\* optimized geometries for rotational transition structures **10** and **11**, formylcyclobutenone (**12**), and inward (**13**) and outward (**14**) transition states for ring opening of **12**. Dihedral angles are the following: **10** C<sub>1</sub>-C<sub>2</sub>-C<sub>3</sub>-C<sub>4</sub> = 85.0°, C<sub>2</sub>-C<sub>3</sub>-C<sub>4</sub>-C<sub>5</sub> = 0.4°; **11** C<sub>2</sub>-C<sub>3</sub>-C<sub>4</sub>-C<sub>5</sub> = 32.0°, C<sub>3</sub>-C<sub>4</sub>-C<sub>5</sub>-O<sub>5</sub> = 91.5°; **13** C<sub>1</sub>-C<sub>2</sub>-C<sub>3</sub>-C<sub>4</sub> = 24.7°, C<sub>2</sub>-C<sub>3</sub>-C<sub>4</sub>-C<sub>5</sub> = 60.6°, C<sub>3</sub>-C<sub>4</sub>-C<sub>5</sub>-O<sub>5</sub> = 18.6°; and **14** C<sub>1</sub>-C<sub>2</sub>-C<sub>3</sub>-C<sub>4</sub> = 21.8°, C<sub>2</sub>-C<sub>3</sub>-C<sub>4</sub>-C<sub>5</sub> = 144.2°, C<sub>3</sub>-C<sub>4</sub>-C<sub>5</sub>-O<sub>5</sub> = 7.7°.

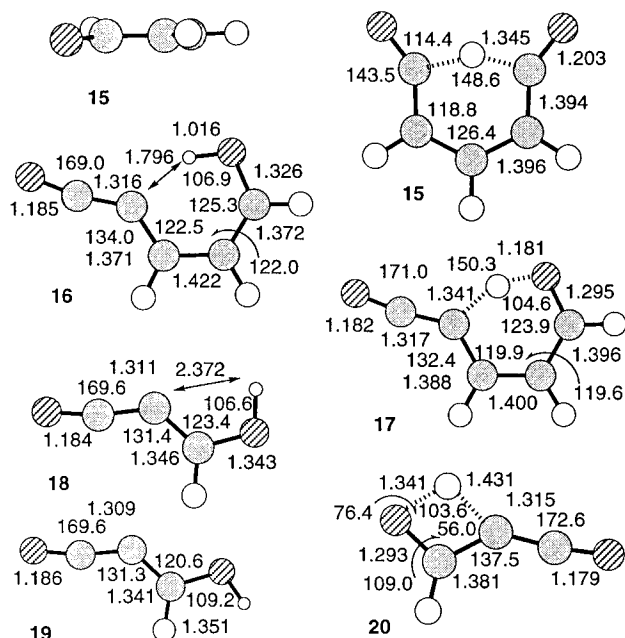
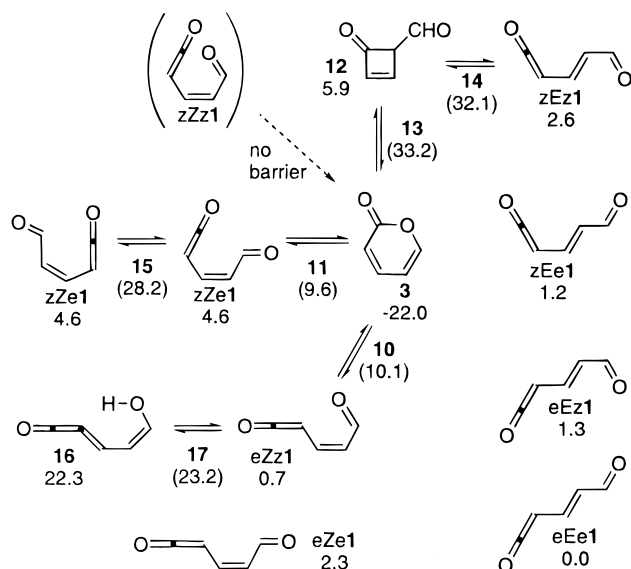


**Figure 3.** MP2/6-31G\* optimized geometries for hydroxyketenes **16**, **18**, and **19** and for hydrogen transfer transition structures **15**, **17**, and **20**. All structures are planar, with the exception of **15**, in which the dihedral angle H<sub>1</sub>-C<sub>1</sub>-C<sub>2</sub>-C<sub>3</sub> is 3.6°.

reaction. These two factors have been suggested to contribute to low barriers in other pseudopericyclic reactions.<sup>4a,b,d</sup> Third, the reaction is exothermic, which, by the Hammond postulate<sup>24</sup> should lead to a lower barrier. This is a rare example of a  $\sigma, \pi$ -aromatization<sup>4d</sup> involving the formation of a single bond, and in this case it would appear that the aromatic stabilization of the product contributes to the low barrier as well. The fourth factor is unique to zZz1, namely that the geometry holds

(24) Hammond, G. S. *J. Am. Chem. Soc.* **1955**, *77*, 334.

Scheme 1



Energies in kcal/mol relative to eEe1. Energies of transition states in parentheses.

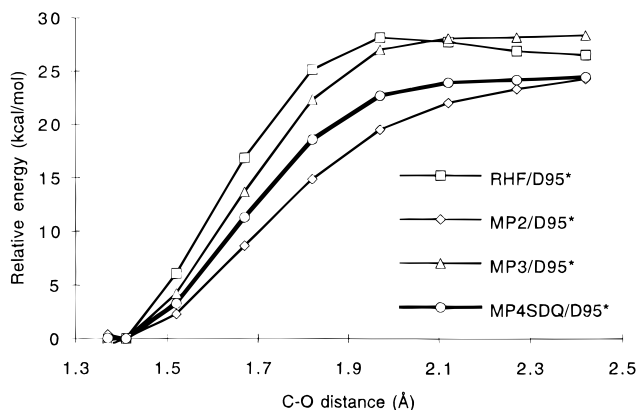


**Figure 4.** Energies of the constrained optimization for the planar ring opening of **3** to **zZz1**. The  $C_1-O_5$  distance was constrained as indicated, and the remainder of the molecule was optimized at the MP2/6-31G\* level. Distortions out of the plane raised the energy. The energy was then calculated at the levels shown. Only at the RHF level is there a minimum corresponding to **zZz1**.

the aldehyde oxygen in very close proximity to the ketene carbon (2.417 Å at the RHF/6-31G\* level) and along the appropriate trajectory for the reaction ( $O_1C_1O_5$  angle of  $97.3^\circ$ , *vide infra*).

Since **zZz1** does not exist, the species observed in argon matrices and in flash photolysis studies<sup>1a,b,f</sup> must therefore be one or more of the other conformations of **1**. Table 2 lists the vibrational frequencies calculated for each. The ketene stretches have been scaled by 0.960, which was shown by Kappe et al. to give excellent agreement with the IR absorptions of acetylketene.<sup>2g</sup> The calculated frequencies are within  $6\text{ cm}^{-1}$  of each other, ranging only from 2124 to 2130  $\text{cm}^{-1}$ . This contrasts with the matrix spectra in which the absorptions range from 2122 to 2146  $\text{cm}^{-1}$ . However, it is likely that the experimental absorptions are doubled by matrix site effects as observed for acetylketene.<sup>2g,8</sup> Thus the presence of four (or five?) ketene peaks does not require the presence of any of the *E* double bond isomers but probably does indicate the presence of at least three conformers.<sup>1a,b</sup>

**Table 2.** Ketene and Carbonyl Stretches of Conformers of **1**<sup>a</sup>

conformation	ketene	carbonyl
zZe1	2124	1640
eZz1	2124	1643
eZe1	2130	1645
zEz1	2124	1658
zEe1	2126	1657
eEz1	2129	1657
eEe1	2129	1656

<sup>a</sup> Calculated at the MP2/6-31G\* level and scaled by 0.960 (reference 2g) and 0.9427 (reference 19) respectively. These scalings give excellent agreement between the experimental and MP2/6-31G\* frequencies for acetylketene (reference 2g).

The carbonyl stretches in table 2 have been scaled by the more general 0.9427 recommended by Pople et al.,<sup>19</sup> although this scale factor does not give exact agreement with experimental values, the trends in frequencies should be well reproduced by the MP2/6-31G\* level.<sup>2g</sup> These calculated absorptions have a broader range, from 1640 to 1658  $\text{cm}^{-1}$ . However, the absorptions in the *Z* family are within  $6\text{ cm}^{-1}$  of each other, 1640–1645  $\text{cm}^{-1}$ , and those of the *E* family are within a range of  $3\text{ cm}^{-1}$ , 1656–1658  $\text{cm}^{-1}$ . The experimental spectra only show two absorptions, at 1690 and 1695  $\text{cm}^{-1}$ , the spacing of which would be consistent with the absorptions of the *Z* family but not from both families. Thus, the experimental ketene and carbonyl absorptions are consistent with the presence of the three *Z* conformers (**zZe1**, **eZz1**, and **eZe1**), if there are indeed multiple ketene peaks due to different matrix sites. While the evidence is not conclusive, we favor this interpretation, in part because the barriers for double bond *Z* to *E* interconversion appear to be quite high, while those for single bond rotations are calculated to be easily surmounted thermally at room temperature and presumably photochemically in a matrix (*vide infra*). Further matrix experiments would be useful to elucidate this point. Alternative precursors might enable the experimental observation of some or all of the *E* double bond conformations of **1**.

Although the various conformations of **1** have not been identified, and the low barriers for reversion to **3** (*vide infra*) makes it unlikely that the relative energies may be experimentally determined, it is instructive to discuss the relative energies of these species (Scheme 1). We have previously shown that the energies of  $\alpha$ -oxoketene conformers do not correlate with the dipole moment.<sup>4c</sup> (This is the case for other molecules.<sup>25</sup> Solvation energies are affected by dipole moments<sup>2g</sup>.) This is true here as well. For example, **zEz1** has the lowest dipole moment ( $2.81\ \mu$ ), but the second highest relative energy (2.6 kcal/mol) as compared to **eEe1**. The trends in relative energies, with an *E*  $C_2-C_3$  double bond are straightforward. In this case, an *s-E* conformation around a single bond (**zEe1** and **eEz1**) is more stable than an *s-Z* by approximately 1.3 kcal/mol<sup>26</sup> and this is additive for **zEz1**, which is 2.6 kcal/mol less stable than **eEe1**. In general, the *Z* conformation around the  $C_2-C_3$  double bond would be expected to be less stable than the *E* and this is the case for **eZe1** which is 2.3 kcal/mol above **eEe1**. However, **zZe1** and **eZz1** are complicated by additional factors. In the former, there is a repulsion between  $C_1$  and  $H_5$  which

(25) Wiberg, K. B.; Laidig, K. E. *J. Am. Chem. Soc.* **1988**, *110*, 1872–1874.

(26) *s-Z*-acrolein is 1.5 kcal/mol higher in energy than *s-E* (MP3/6-311++G\*\*/MP2/6-31G\*).<sup>27</sup> Likewise *s-Z*-vinylketene is 1.6 kcal/mol higher than *s-E* (MP4(SDQ)/6-31G\*\* + ZPE)<sup>10a</sup>

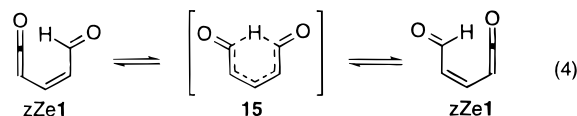
is manifest in the nonplanarity of the molecule (Figure 1) and the high relative energy (4.6 kcal/mol). This is in part an electrostatic interaction, since the two atoms each bear a partial positive charge. On the other hand, the stability of *eZz1* is due to an attractive interaction between H<sub>2</sub> and O<sub>5</sub> as evidenced by the slightly longer C<sub>5</sub>–O<sub>5</sub> bond in *eZz1* (1.236 Å) as compared to the other conformations (1.230 Å to 1.232 Å.) The low dipole moment of only 2.83 μ also contributes to the stability of this conformer. The other aspects of the geometries of these structures are unremarkable.

**Interconversions and Cyclizations of 1.** The question then arises, how do the seven conformers of **1** (Scheme 1) interconvert and form pyran-2-one (**3**)? Rotations around single bonds in *zZe1* and *eZz1* should both lead directly to **3**, and two true transition structures (**10** and **11**) indeed were located at the MP2/6-31G\* level and are shown in Figure 2. These occur at dihedral angles of 85.0° and 91.5° respectively. Interestingly, although the remainder of the molecule is essentially planar in **10**; the C<sub>1</sub>–C<sub>2</sub>–C<sub>3</sub>–C<sub>4</sub> dihedral angle is twisted to 32.0° in **11**. This may be related to the original nonplanarity of *zZe1* (Figure 1). The C<sub>1</sub>–O<sub>5</sub> distances are quite long (3.364 Å and 3.140 Å, respectively) suggesting little bonding at the transition states. The potential energy surface in the vicinity of *zZz1* is best described as a potential energy “chute”. As the molecule rotates from *zZe1* or *eZz1* and passes over the barrier and enters this chute which is downhill toward **3** and uphill in all other directions. Only after entering the chute does it experience C<sub>1</sub>–O<sub>5</sub> bonding.

These calculated rotational barrier heights should be related to the experimental rates of disappearance of (an) unspecified conformer(s) of **1**. Half-lives have been reported to be 2.9 μs (presumably) at room temperature<sup>1f</sup> and 0.92 μs at 45.7 °C.<sup>1c</sup> Taken at face value, these give an *E<sub>a</sub>* of 10 kcal/mol, which may be compared with the calculated barriers under two different scenarios. If equilibration between the various conformations is slow, then the calculated barrier from *eZz1* to **3** is 9.3 kcal/mol and from *zZe1* to **3** is 5.0 kcal/mol, respectively. In this case, the reaction observed would be the conversion of *eZz1* to **3** while the room temperature rotation from *zZe1* was faster than could have been detected because of the substantially lower barrier. Alternatively, if interconversion between the conformers is rapid, the rate limiting step would be the rotation from *zZe1* to **3**, the barrier to which, via **11**, is calculated to be 8.9 kcal/mol above *eZz1*. In either scenario, the calculated barriers are in reasonable agreement with the experimental rates. Experimental discrimination between these two mechanistic scenarios would appear to be challenging. Computational discrimination between them would have required calculation of all possible rotational transition states; this was not attempted due to the magnitude of the task in proportion to the limited insight expected. Nonetheless, the lack of products from methanol trapping of **1**<sup>1f,28</sup> can be attributed to the availability of low energy pathways for cyclization to **3** and to the lack of a pseudopericyclic pathway for the addition of methanol to **1**, while the [2 + 2] addition of methanol would be expected to have a much higher barrier.<sup>29</sup>

Despite numerous attempts, no transition state for a direct interconversion between the *Z* and *E* olefin conformational families could be located. However, this search did lead to two pericyclic transition states (**13** and **14**, inward and outward, 27.4 and 26.3 kcal/mol above **12**, respectively) for the conrotatory electrocyclic ring opening of the apparently unknown 4-formyl-2-cyclobutenone (**12**).<sup>30</sup> The nonplanarity of the opening rings (C<sub>1</sub>–C<sub>2</sub>–C<sub>3</sub>–C<sub>4</sub> dihedral angles of 24.7° and 21.8°, respectively), typical for pericyclic ring openings<sup>31</sup> contrasts with the planar transition structure calculated for the pseudopericyclic ring opening of oxetone to **2**.<sup>4b,10a</sup> The torquoselectivity favors outward rotation instead of the inward found for formylcyclobutene,<sup>31b</sup> in part because C<sub>1</sub> is electron deficient. A preference for inward rotation might also have been expected if C<sub>1</sub>–O<sub>5</sub> bonding in **13** were important. (The C<sub>1</sub>–O<sub>5</sub> bond length in **13** is 2.791 Å.) However, this bonding involves pericyclic orbital overlap, which can increase the barriers to reactions as compared to pseudopericyclic ones.<sup>4d</sup> The strain in **12** places it higher in energy than any of the ketene conformations but the high barriers suggest it should be amenable to synthesis. Overall, a thermal mechanism for the conversion of *zZe1* to pyran-2-one (**3**) is provided by transition structures **14** and **13**, via **12** (Scheme 1). However, at 27.4 and 26.3 kcal/mol above **12**, respectively, the barriers are too high for **12** to be involved in the rapid room temperature thermal disappearance of **1**.<sup>1f</sup>

**Hydrogen Transfer Reactions.** The transition state for the degenerate 1,5-sigmatropic hydrogen migration of *zZe1* (eq 4 and Scheme 1) was anticipated to be planar, in analogy with the hydrogen migration in the enol of malonaldehyde,<sup>32</sup> which may also be viewed as pseudopericyclic. Although a planar (*C<sub>2v</sub>*) structure was a true transition structure at the RHF/6-31G\* level, it had two imaginary frequencies at the MP2/6-31G\* level (–423.9 and –131.1 cm<sup>–1</sup>), the first corresponding to hydrogen migration and the second corresponding to a weak out-of-plane motion. The reoptimized transition state **15** with lower (*C<sub>s</sub>*) symmetry was nearly planar (the H–C–C–C dihedral angle was only 3.6°, see Figure 3) and only 0.03 kcal/mol lower in energy than the planar one at the MP2/6-31G\* level. Because of a concern that the basis set might not be adequately flexible, the structures were reoptimized at the MP2/6-31++G\*\* level. The *C<sub>s</sub>* structure was again more stable (by 0.11 kcal/mol) than the planar one. Single point energies with the D95\*\* basis set were carried out on both sets of structures; in this case, with the exception of the MP3/D95\*\* level, the planar structure was always calculated to be more stable than the nonplanar one.



The calculated barrier to the hydrogen migration is high, 39.2 kcal/mol (MP4(full, SDTQ)/D95\*\* + ZPE) above pyran-2-one (**3**) and 27.9 kcal/mol (MP4(full, SDQ)/D95\*\* + ZPE) above *eZz1*. The inclusion of triple

(30) Two additional transition states, inward and outward, in which the formyl group of the ketenes will be trans, are also expected.

(31) (a) Spellmeyer, D. C.; Houk, K. N. *J. Am. Chem. Soc.* **1988**, *110*, 3412. (b) Rudolf, K.; Spellmeyer, D. C.; Houk, K. N. *J. Org. Chem.* **1987**, *52*, 3708–3710.

(32) Frisch, M. J.; Scheiner, A. C.; Schaefer, H. F., III. *J. Chem. Phys.* **1985**, *82*, 4194–4198.

(27) Wiberg, K. B.; Rosenberg, R. E.; Rablen, P. R. *J. Am. Chem. Soc.* **1991**, *113*, 2890–2898.

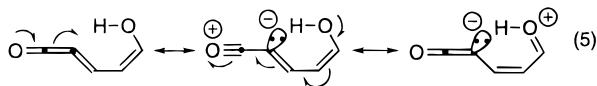
(28) McIntosh, C. L.; Chapman, O. L. *J. Am. Chem. Soc.* **1973**, *95*, 247–248.

(29) Duan, X.; Page, M. *J. Am. Chem. Soc.* **1995**, *117*, 5144–5119.

excitations lowered this barrier significantly (Table 1). The barrier height is consistent with that required for the rearrangement of **5** to occur at 650 °C,<sup>1c</sup> within the short contact time of flash vacuum pyrolysis. The origin of this barrier will be discussed in more detail below.

The hypothetical proton transfer from *s*-*Z*,*Z*-5-hydroxy-1,2,4-pentatrien-1-one (**16**) to form eZz1 (Scheme 1) was studied as a further example of a pseudopericyclic hydrogen transfer reaction. To the best of our knowledge, this cumulene is as yet unknown, although the nitrogen analog exists in equilibrium with imidoalkene.<sup>15,33</sup> The optimized geometry of **16** is shown in Figure 3. The C<sub>1</sub>–C<sub>2</sub>–C<sub>3</sub> angle is far from linear in both the RHF/6-31G\* and MP2/6-31G\* geometries; it is 134.0° in the latter. This is a remarkable distortion. Extended cumulenes may be nonlinear,<sup>34</sup> and although RHF theory does not always reproduce the experimental geometry, MP2/6-31G\* calculations do.<sup>34</sup> Analogs of carbon suboxide tend to have very flat bending potentials.<sup>34</sup> In the case of **16**, however, the relatively large magnitude of the lowest vibrational frequency (118.1 cm<sup>-1</sup> as compared to 80 cm<sup>-1</sup> in iminopropadienone<sup>34b</sup>) and the agreement between the RHF and MP2 geometries suggest the potential well is well defined.

The shorter homologs, *s*-*Z*- and *s*-*E*,*cis*-3-hydroxy-1,2-propadien-1-one (**18** and **19**) were then examined. Both isomers exhibited a similar bend (131.4° and 134.3°, respectively). The latter structure rules out a hydrogen bond or incipient proton transfer as the origin of the bend in **16** and **18**. Rather, it would appear that the bend in all three structures is due to an electronic effect of the hydroxyl oxygen. From a resonance point of view, in-plane electron donation from O<sub>1</sub> in **16**, (as well as in **18** and **19**) would increase the electron density at C<sub>2</sub>. However, out-of-plane donation from O<sub>5</sub> would then reduce the positive charge on O<sub>1</sub>, as shown in eq 5. The charge on C<sub>2</sub> is stabilized in the sp<sup>2</sup> orbital formed by rehybridization of the carbon.<sup>35</sup> More generally, this analysis suggests that any oxocumulene with an electron-donating substituent should have a similar bend. This is the case for difluoropropadienone, with a calculated C–C–C angle of 132.8° at the RHF/6-31G\* level.<sup>37</sup>



3-Hydroxy-1,2-propadiene-1-one (**18** or **19**) has been produced in argon matrices by the photolysis of formylketene **2**,<sup>9b</sup> although the conformation of the hydroxyl group was not discussed, nor was the bend anticipated. The IR absorptions at 3526, 2128, and 1692 cm<sup>-1</sup> were assigned to the OH, cumulene, and C=C stretches of this molecule. These are compared to the scaled calculated frequencies for **18** and **19** in Table 3. The experimental

**Table 3. Comparison of Selected, Calculated IR Absorptions for *Z* and *E*-3-Hydroxy-1,2-propadien-1-one with Those Experimentally Observed<sup>a</sup>**

calculated <b>18</b>	calculated <b>19</b>	observed
3456.6	3531.9	3526
2111.9	2112.9	2128
1659.3	1680.4	1692

<sup>a</sup> Calculated absorptions were scaled by 0.9427 (reference 19).

OH and C=C stretches clearly are closer to the frequencies calculated for the *E* rotamer. Thus we assign the experimentally observed spectrum to **19**, despite the fact that it is calculated to be higher in energy than **18**.<sup>38</sup> The agreement between the calculated and experimental IR spectra provides indirect support for the bent geometry. In view of the dramatically bent geometries of **18** and **19**, and in light of the substantial barrier for isomerization to **2** (*vide infra*), a structural determination would be a worthwhile and attainable experimental goal.

The transition structure **17** for the hydrogen transfer from **16** to form eZz1 is shown in Figure 3. The barrier to this reaction is remarkably low, only 0.8 kcal/mol. The transition structure **20** for the homologous hydrogen transfer from **18** to formylketene **2** is also shown in Figure 3. Both structures are planar, as anticipated for pseudopericyclic reactions, although the barrier for the latter proton transfer is much larger, 29.8 kcal/mol. The exothermicities for the two reactions are comparable, 21.6 kcal/mol for the first system and 20.2 kcal/mol for the second (Table 1, MP4(full, SDTQ)/D95\*\* + ZPE). The patterns of electrophilicity and nucleophilicity are likewise similar. Although it might seem appropriate to describe the more difficult reaction as forbidden, it is more consistent to attribute the differences in barrier height to the differences in the geometry of hydrogen transfer, as argued below.

**Origins of Barriers to Pseudopericyclic Hydrogen Transfer.** Barriers to hydrogen transfer in other systems have been shown to be affected by the geometry of the transfer and by the identity of the atoms between which the hydrogen moves.<sup>39</sup> For this discussion, comparisons will be limited to transfers between identical atoms so that only the geometries and the number of atoms in the ring are varied. Only three assumptions need to be made to qualitatively rationalize the trends in reactivities in the hydrogen transfer reactions discussed above. (1) Hydrogen transfers most readily along a linear path.<sup>39a,c</sup> (2) Proton transfer to or from an oxygen occurs most readily at X–O–H angles around 115–120°. <sup>39b</sup> (3) Hydrogen transfer to the central carbon of a ketene is preferred at a H–C–O angle of approximately 120°, in analogy to the Burgi–Dunitz trajectory for nucleophilic addition to carbonyls.<sup>40,41</sup> These preferred angles are indicated in Figure 5 for each of the reactions discussed below.

First consider the 1,5-hydrogen transfer in malonaldehyde; the barrier for this thermoneutral reaction is

(38) It may be that **18**, although the thermal barrier is significant, isomerizes with a high quantum yield to **2** and so is not observed in the matrix.

(39) (a) Hillenbrand, E. A.; Scheiner, S. *J. Am. Chem. Soc.* **1986**, *108*, 7178–7186. (b) Cybulski, S. M.; Scheiner, S. *J. Am. Chem. Soc.* **1989**, *111*, 23–31. (c) Duan, X.; Scheiner, S. *J. Am. Chem. Soc.* **1992**, *114*, 5849–5856.

(40) Burgi, H. B.; Dunitz, J. D.; Shefter, E. *J. Am. Chem. Soc.* **1973**, *95*, 5065–5067.

(41) Efforts are underway to explore this question in more detail.

(33) Cheikh, A. B.; Chucho, J.; Manisse, N.; Pommelet, J. C.; Netsch, K.-P.; Lorencak, P.; Wentrup, C. *J. Org. Chem.* **1991**, *56*, 970–975.

(34) (a) Brown, R. D.; Champion, R.; Elmes, P. S.; Godfrey, P. D. *J. Am. Chem. Soc.* **1985**, *107*, 4109–4112. (b) Mosandl, T.; Stadtmüller, S.; Wong, M. W.; Wentrup, C. *J. Phys. Chem.* **1994**, *98*, 1080–1086.

(35) The bending of cumulenes has also been discussed in terms of the valence bond interaction of their fragments. In this light, **18** and **19** can be considered as the interaction of carbon monoxide with the carbene hydroxyvinylidene.<sup>36</sup> This would also predict a bent geometry.

(36) Trinquier, G.; Malrieu, J.-P. *J. Am. Chem. Soc.* **1987**, *109*, 5303–5315.

(37) (a) Brahm, J. C.; Dailey, W. P. *J. Am. Chem. Soc.* **1989**, *111*, 8940–8941. (b) Brahm, J. C.; Dailey, W. P. *J. Am. Chem. Soc.* **1989**, *111*, 3071–3073.

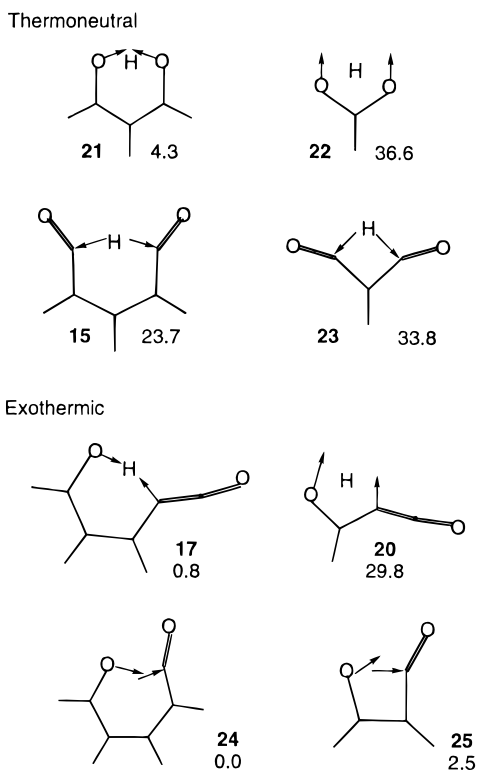


**Figure 5.** Preferred geometries of attack at pseudopericyclic transition structures. The drawings are of the MP2/6-31G\* transition structures and are to scale. The arrows are drawn from nucleophile to electrophile and show the postulated preferred angles of attack on the carbonyls ( $\angle \text{H-O-C} = 115^\circ$  in **21** and **22**) and the ketenes ( $\angle \text{O-C-H} = 120^\circ$  in **15** and **23**,  $\angle \text{C-C-H} = 120^\circ$  in **17** and **20**, and  $\angle \text{O-C-H} = 120^\circ$  in **24** and **25**.) The activation energies are shown in kcal/mol and are from this work, except **21** (MP4(SDTQ)/6-31G\*\*//MP2/6-31G\*\*, reference 32), **23** (G2(MP2), reference 10c), and **25**, (MP4(SDQ)/6-31G\*\*//MP2/6-31G\*, reference 4b).

calculated to be only 4.3 kcal/mol at the MP4/6-31G\*\*//MP2/6-31G\*\* level.<sup>32</sup> On the other hand, the barrier to 1,3-hydrogen migration in formic acid<sup>42</sup> is calculated here to be 36.6 kcal/mol (MP4(full, SDTQ)/D95\*\* + ZPE). The O-H-O angle at the malonaldehyde transition state (**21**, MP2/6-31G\*\* level) is  $157.8^\circ$ , while for formic acid (**22**, MP2/6-31G\* level, this work) it is  $105.5^\circ$ . The H-O-C angle in the former is  $101.2^\circ$  and in the latter it is  $71.0^\circ$ . The degree of distortion clearly correlates with the barrier height. The transition state **22** resembles that for proton transfer between the amines in protonated diaminomethane, which is also planar and in which the N-H-N angle of  $111.3^\circ$  is similarly quite distorted away from linear.<sup>39c</sup> This parallel is expected for a pseudopericyclic reaction, in which the proton is transferred from one lone pair to another in plane in **22**, while the out-of-plane  $\pi$ -system merely serves as a wire to maintain electron balance.

A similar comparison can be made between the 1,5-sigmatropic hydrogen migration via transition structure **15** and that calculated for the analogous 1,3-shift in formylketene.<sup>10a,c</sup> The barrier in the 1,5-shift from the ketene zZe1 is 23.7 kcal/mol. The MP4(SDQ)/6-31G\*\*//RHF/6-31G\*\* barrier for the 1,3-shift in formylketene is 39.7 kcal/mol,<sup>10a</sup> while at the G2(MP2) level, it is 33.8 kcal/mol.<sup>10c</sup> Both of these are thermoneutral reactions; both geometries are reasonably appropriate for hydrogen

transfer to the ketene carbon; the O-C-H angle in **23** (MP2/6-31G\*)<sup>10c</sup> is  $121.8^\circ$  while in **15** it is  $114.4^\circ$ . This angle in **15** is slightly smaller than ideal because there is insufficient space for the linear C-H-C bond between the two carbons. This also leads to the small out-of-plane distortion (*vide supra*). However, the geometry on the hydrogen being transferred is poorer in the 1,3-shift. The C-H-C angle in **23** is  $90.7^\circ$ , which is greatly distorted from linear, while the same angle in **15**, at  $148.6^\circ$ , is less distorted. This distortion from the ideal geometry in **23** makes the barrier higher than for **15**.

Why is the barrier for hydrogen transfer in **15** so much higher than in malonaldehyde (**21**)? Both transition states have only minor distortions from the ideal geometries for hydrogen transfer. However, in malonaldehyde, hydrogen is being transferred to an electron rich atom, while in **15** the transfer is to an electron deficient center. The same is true in the transfer to an electron deficient carbon of the ketene in **23** as compared to the electron rich oxygen **22**.

The question can be asked in a different perspective: Why is the barrier for proton transfer in formic acid (**22**) so much higher (34 kcal/mol) than in malonaldehyde (**21**), while hydride transfer in **23** is only 16 kcal/mol higher than in **15**? There is slightly less distortion in the O-H-O angle in **22** ( $105.5^\circ$ ) than there is in the C-H-C angle **23** ( $90.7^\circ$ ) because O-H bonds are shorter than C-H bonds. However, there is much more distortion in the C-O-H angle in **22** ( $71.0^\circ$ ) than in the O-C-H angle in **23** ( $118^\circ$ ) because the bending of the ketene in **23** aims the hydrogen at the ketene along the preferred angle of attack, while in **22**, the preferred angle of attack on the oxygens points away from the hydrogen. Thus in the oxygen series, the four-centered transition state **22** has a much worse geometry than the six-centered **21**, while in the ketene series, the geometry of **20**, while less favorable than **15**, is not that much worse and the barrier is not dramatically higher.

The same principles apply to the six-centered transition structure **17**, in which the C-H-O angle is  $150.3^\circ$  and the H-O<sub>5</sub>-C<sub>5</sub> angle is  $104.6^\circ$  and to the four-centered transition state **20**, in which the C-H-O angle of  $103.6^\circ$  is significantly distorted away from linearity and at  $76.4^\circ$ , the H-O-C angle is similarly compressed. The C<sub>1</sub>-C<sub>2</sub>-H angle in **17** is  $126^\circ$ , while it is only  $56.0^\circ$  in **20**. It seems reasonable that these gross distortions away from the preferred geometries could lead to the observed 29 kcal/mol difference in barrier heights.

Finally, the barriers to ring closure of zZz1 via **24** (*vide supra*) and ring opening of oxetone to **2** via **25**<sup>4b,d</sup> are nonexistent and only 2.5 kcal/mol, respectively. The low magnitude of each reflects the exothermicities of both reactions, the favorable electrophilicities and nucleophilicities of the reactants, as previously argued,<sup>4b,d</sup> but also the favorable reaction geometries in each case. Most dramatically, however, *both* the barriers are very low, regardless of the number of electrons involved.

## Conclusions

Geometries have been obtained for the conformers of 5-oxo-2,4-pentadienal (**1**) at the MP2/6-31G\* level, as well as several related species and transition states between them. Energies have been determined at the MP4(full, SDQ)/D95\*\* + ZPE level. These results indicate that one of the potential conformers of **1** (zZz1) does not exist. The multiple ketene peaks observed in argon matrices and

(42) Nguyen, M. T. *Chem. Phys. Lett.* **1989**, *163*, 344-348.



previously assigned to four conformers of **1** are now assigned to only three of these conformers, *zZe1*, *eZz1*, and *eZe1*, while the extra absorptions are tentatively attributed to matrix effects. The calculated rotational barriers (via **10** and **11**) are consistent with the observed rates of disappearance of **1**. Interconversion of the double bond isomers of **1** is suggested to proceed via inward (**13**) and outward (**14**) electrocyclic ring openings of formylcyclobutenone (**12**). An experimental reinvestigation of this system, as well as studies of alternative precursors to **1** would appear to be warranted.

The experimentally observed IR spectrum of 3-hydroxy-1,2-propadienone is assigned to the less stable *E* rotamer **19**, by comparison with the calculated IR spectra of the *E* and *Z* rotamers. These two cumulenes are strongly bent, indicating near  $sp^2$  hybridization at  $C_2$ . The high barrier to proton transfer suggests the structure of this molecule could be determined experimentally. The vinylogous cumulene **16** is also predicted to be significantly bent ( $134.0^\circ$ ) but is unlikely to be observed because the barrier to proton transfer (without tunneling) is calculated to be only 0.8 kcal/mol. The methoxy analog could probably be observed because methyl transfer is more difficult than proton transfer.

The barrier heights have been discussed in terms of the pseudopericyclic reaction model, in which the lack of overlap between  $\sigma$  and  $\pi$  orbitals leads to all reactions being orbital symmetry allowed. This offers an explanation for both the nonexistent barrier to the ring closure of *zZz1* and the very low (2.5 kcal/mol) barrier to ring opening of oxetone (**9**) to **2**, despite the differing number of electrons involved. It has been argued that the transition structures for pseudopericyclic reactions are usually planar and the barriers can be very low, in some

cases lower than a competing pericyclic pathway.<sup>4b,d</sup> However, as this work demonstrates, the actual barrier height will depend on (1) the exothermicity of the reaction, (2) the electrophilicity/nucleophilicity match between the reacting centers, and (3) the detailed geometry of the forming bonds. A more quantitative analysis of these factors is underway, and reports on additional pseudopericyclic reactions will follow in due course.

**Acknowledgment.** This work was supported by a grant from the Robert A. Welch Foundation. Some of the calculations were carried out at the Pittsburgh Supercomputing Center, under Grant number CHE-930031P.

**Note Added In Proof.** Sannes and Brauman have recently argued that the facile 1,3-hydrogen shift in the enolate of acetone is orbital symmetry allowed via a planar transition state. The rotation which prevents cyclic orbital overlap also makes this a pseudopericyclic reaction. Sannes, K. A.; Brauman, J. I. *J. Am. Chem. Soc.* **1995**, *117*, 10088–10092.

**Supporting Information Available:** MP2/6-31G\* optimized Cartesian coordinates and vibrational frequencies for all stationary points, a table of energies for single point calculations reported in Figure 4, a table of absolute energies calculated for all stationary points, and a figure showing the orbitals involved in the degenerate 1,5-hydrogen shift of *zZe1* (12 pages). This material is contained in libraries on microfiche, immediately follows this article in the microfilm version of the journal, can be ordered from the ACS, and can be downloaded from the Internet; see any current masthead page for ordering information and Internet access instructions.

JO951716T